Mass-Analyzed Threshold Ionization Spectroscopy of 2-Phenylethanol: Probing of Conformational Changes Caused by Ionization

S. Georgiev, R. Karaminkov, S. Chervenkov,† V. Delchev,‡ and H. J. Neusser*

Physikalische und Theoretische Chemie, Technische Universität München, Lichtenbergstrasse 4, 85748 Garching, Germany

Received: May 29, 2009; Revised Manuscript Received: September 9, 2009

The vibrational structure of the ionic ground state of different conformers of the biologically relevant molecule 2-phenylethanol has been investigated by combination of two-photon two-color mass-analyzed threshold ionization spectroscopy (MATI) and quantum chemical calculations at M05, MP2, and coupled cluster (CC) levels of theory with extended basis sets. MATI spectra recorded via gauche vibronic bands are with poor structure and increasing background, whereas the ones measured via vibronic bands of the anti conformers feature well-resolved vibronic structure in the cation. Ab initio computations predict three stable conformers for the 2-phenylethanol cation out of five initial neutral structures. None of the theoretical structures in the cation features a nonclassical OH$\cdots\pi$ hydrogen bond in conjunction with the analysis of the MATI spectra. This provides clear evidence that the OH$\cdots\pi$ hydrogen bond stabilizing the lowest-energy gauche conformer in the neutral breaks upon ionization.

I. Introduction

In recent years, great interest has been invoked in the study of neutral and ionic biologically relevant molecules and their hydrogen-bonded complexes with water or small organic species.[1−10] Such molecules act as chromophores in proteins, nucleic acids, and neurotransmitters as they are responsible for the absorption in the near-UV region. Their spectroscopic investigation helps to understand the mechanisms leading to conformational changes upon excitation and ionization[3−7] as well as the formation of hydrogen bonds of different types and strengths in many biochemical molecular systems. In addition, molecular ions play a crucial role in many processes in the living cell, and their study reveals the possible pathways of many biochemical reactions.

Conventional time-of-flight photoelectron spectroscopy leads to a resolution of about 10 meV, which, for large molecular ions, is not sufficient to resolve their low-frequency vibrational bands below 100 cm^{-1}.[7,11] An improvement of the energy resolution has been achieved with techniques based on threshold ionization zero-electron kinetic energy (ZEKE)[12] and mass-analyzed threshold ionization (MATI).[13−15] These methods have been successfully applied in recent years for the study of various biologically relevant molecules and their van der Waals and hydrogen-bonded complexes.[3−6,16,17]

In this work, we extend our investigation to flexible molecules by studying the ground cationic state of 2-phenylethanol (2-PE) (see Scheme 1). 2-Phenylethanol has been previously studied by a variety of spectroscopic techniques, UV and UV ion-dip spectroscopy experiments,[18] millimeter-wave spectroscopy,[19] infrared−ultraviolet double resonance spectroscopy,[20] laser-induced fluorescence excitation, and mass-selected resonant two-photon ionization (R2PI) experiments,[21] and has recently been complimented by a high-resolution UV rotationally resolved experiment carried out by our group with an assignment of the observed rovibronic bands and the identification of two conformers.[22] These studies were focused on the structure, conformational diversity, and bonding of 2-PE either in the electronic ground, S_0, state or in the first excited, S_1, state and supported by ab initio calculations. While these investigations provided information on the neutral molecule, Weinkauf et al.[7] reported multiphoton ionization photoelectron spectra of 2-PE yielding experimental results on the cationic ground state of this molecule. In this work, we present the first threshold ionization spectra of 2-PE with high resolution ($\sim$5 cm^{-1}) achieved with the MATI technique. MATI spectra were measured via the gauche electronic origin at 37 622 cm^{-1} and two other bands in the S_1 intermediate state lying at 48 and 58 cm^{-1} relative to the gauche electronic origin. The first of these peaks (48 cm^{-1}) was unambiguously assigned to an anti conformer,[22] while the conformer giving rise to the 58 cm^{-1} peak is not yet conclusively identified.

SCHEME 1: Atom Labels of the 2-PE Monomer

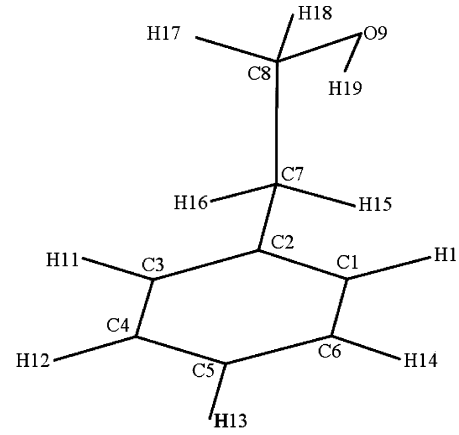

The interpretation of our results will focus on unveiling the nature of the peak at 58 cm^{-1} in the $S_1 \leftarrow S_0$ excitation spectrum

* To whom correspondence should be addressed. E-mail: neusser@ch.tum.de.

† Present address: Max-Planck-Institut für Quantenoptik, Hans-Kopfermann-Str. 1, D-85748 Garching, Germany.

‡ Permanent address: University of Plovdiv, Dept. Physical Chemistry, Tzar Assen Str. 24, 4000 Plovdiv, Bulgaria.

10.1021/jp908045k CCC: $40.75
Published on Web 10/02/2009

based on comparison between the vibrational profiles in the MATI spectra via the 48 and 58 cm^{-1} bands. The experimental findings for the ionic vibrational frequencies will be compared with the results from ab initio calculations employing the new hybrid functional M05.[23] In this way, we aim at clarifying the role of the intramolecular OH$\cdots\pi$ hydrogen bond in stabilizing the conformational structures and how this bond is affected upon ionization. Furthermore, we investigate the effect of fluorine substitution on the $S_1 \leftarrow S_0$ 0_0^0 transition, comparing the experimental and theoretical findings for 2-PE with those for 2-*para*-fluorophenylethanol (2-*p*FPE)[24,25] to elucidate the importance of the OH$\cdots\pi$ bonding on the stabilization of the molecular conformers in the presence of an electron-withdrawing atom.

II. Experimental Setup

The threshold ionization methods utilizing pulsed electric field, ZEKE and MATI are based on the excitation of high-lying ($n \gg 100$) long-lived ($\sim\mu$s) Rydberg states in atoms and molecules. It has been shown by our group[26] that Rydberg states in the region of $40 \leq n \leq 110$ can be resolved in high-resolution optical double resonance experiments.[26] However, higher-lying states that mainly contribute to the ZEKE and MATI signals lie above the Inglis−Teller limit and thus are unresolvable. In this work, the high Rydberg states are excited by a two-photon excitation scheme via various intermediate vibronic S_1 states originating from different conformers.

Then, a pulsed electric field is applied so that the weakly bound Rydberg electrons are detached from the ionic core with nearly no excess energy. As a result, sharp peaks are observed at the individual thresholds. One should, however, bear in mind that the ionization threshold is lowered by the presence of the electric field, which causes shift of the individual thresholds typically by <10 cm^{-1}. In addition, the widths of the resulting peaks in a pulsed field ionization (PFI) spectrum are affected by the application of a pulsed electric field, resulting in a resolution of about 5 cm^{-1} in our experiment.[27] The so-produced threshold ions are detected mass-selectively in a mass spectrometer.

The experimental setup has been described elsewhere.[28] Briefly, it consists of a home-built linear reflectron time-of-flight (RETOF) mass spectrometer[29] and two tunable dye lasers (LPD 3000 and FL 3002, Lambda Physik), synchronously pumped by an excimer XeCl laser (Lambda Physik, EMG 1003i). Both dye lasers are operated with Coumarin 153, and the laser wavelengths are calibrated with a wavemeter (WaveMaster, Coherent). The supersonic molecular beam is produced by the expansion of a gas mixture of 2-PE (Fluka Chemie, 99% purity) vapors and Ar buffer gas through a modified heatable nozzle (General Valve). Before entering the region of interaction with the laser beams, the cold molecular beam is skimmed to reduce the particle density. In order to obtain a suitable 2-PE concentration in the gas phase, the sample is heated to 105 °C. The use of a RETOF mass spectrometer provides high mass resolution, which is important for the study of large molecular ions and complexes. For these molecules, there exist ^{13}C isotopomers with high abundance leading to a dense mass spectrum, which can be mass separated in the reflectron TOF mass spectrometer. In addition, in the supersonic expansion, different complexes of the investigated molecule and the carrier gas or impurities can be produced, leading to a variety of fragments which have to be separated from the investigated mass.

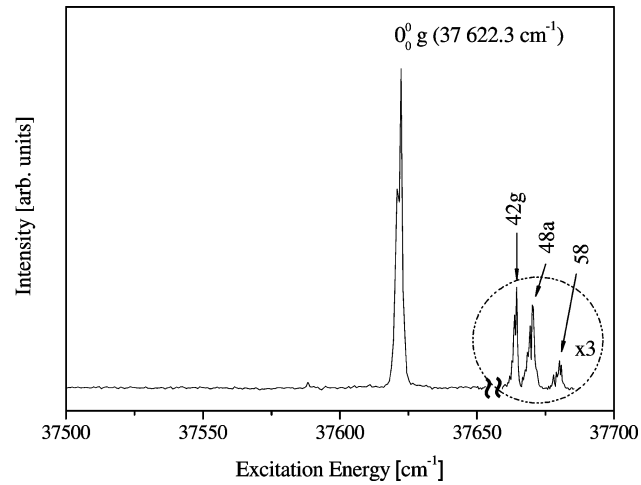

Figure 1. One-color $S_1 \leftarrow S_0$ REMPI spectrum of 2-PE, recorded at the monomer mass channel $m/z = 122$. Conformer assignments and relative peak positions are included in the spectrum. Bands originating from gauche and anti conformers[22] are designated by g and a, respectively.

III. Results

1. REMPI Spectra. The one-color resonance-enhanced multiphoton ionization (REMPI) spectrum of the first excited, S_1, electronic state measured with the setup described above is shown in Figure 1. The REMPI spectrum exhibits the same vibronic profile as the one in our previous publication,[22] where the strongest band at 37 622.3 cm^{-1} was identified as the origin of the gauche conformer, which is stabilized by a OH$\cdots\pi$ hydrogen bond. The peak at 48 cm^{-1} was assigned to the anti conformer of 2-PE.[22] The identification of the additional peak at 58 cm^{-1} is not clear. The small energy gap between the two bands ($\sim$10 cm^{-1}) brings out the interesting issue of whether they originate from the same conformational structure or they can be assigned to the origins of two different anti structures. In our previous work,[22] on the basis of the high-resolution spectra with rotational resolution of the excited, S_1, electronic state, we tentatively assigned them to the same anti conformer in the ground, S_0, electronic state.

2. MATI Spectra. We measured MATI spectra in a two-color excitation scheme via the above-mentioned three intermediate vibronic states in the first excited, S_1, electronic state.

As a first step, we recorded the total ion current spectra (TIC) as a function of the two-photon excitation energy, where the first photon energy is fixed to one of the electronic origins of the two conformers of interest in the S_1 intermediate state. The total ion current measured via the 0_0^0 band (37 622.3 cm^{-1}) of the gauche conformer in the S_1 intermediate state is shown in Figure 2a. It does not exhibit a step-like behavior but a monotonously increasing total ion current signal without discernible thresholds. This makes it hard to estimate an ionization threshold and to identify vibrational levels in the cationic ground state. On the other hand, the TIC signal via the anti origin at 37 670 cm^{-1} (Figure 2b) displays two well-pronounced steps at 71 422 and 71 544 cm^{-1}, indicating the AIE and a low-frequency vibration shifted by approximately 122 cm^{-1}.

Figure 3 displays the threshold ion spectra, when using the two-color excitation scheme, via the electronic origins of the gauche (Figure 3a) and anti (Figure 3b and c) conformers in the S_1 electronic state at 37 622.3, 37 670 (48 cm^{-1} band), and 37 680 cm^{-1} (58 cm^{-1}), respectively. The MATI spectrum of the gauche conformer in Figure 3a does not exhibit the

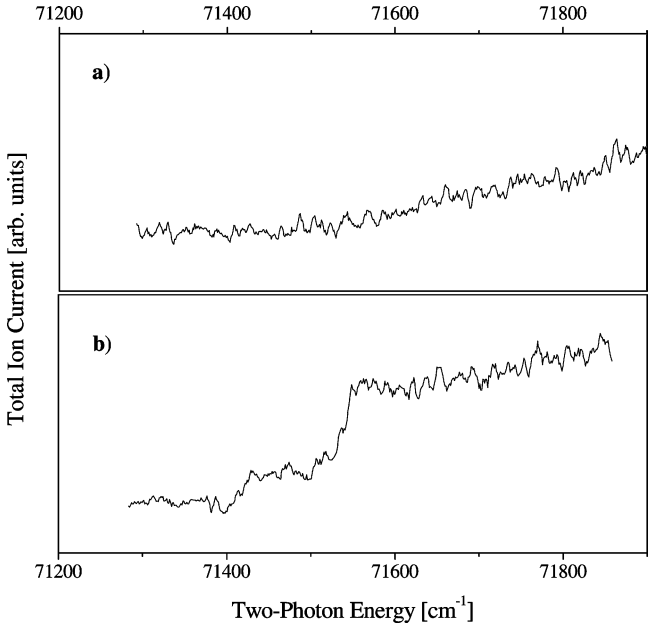

Figure 2. Total ion current spectra of 2-PE measured in a two-color REMPI experiment with the first photon energy fixed to the gauche (a) and anti (b) origins of the two conformers in the S_1 electronic state (see Figure 1).

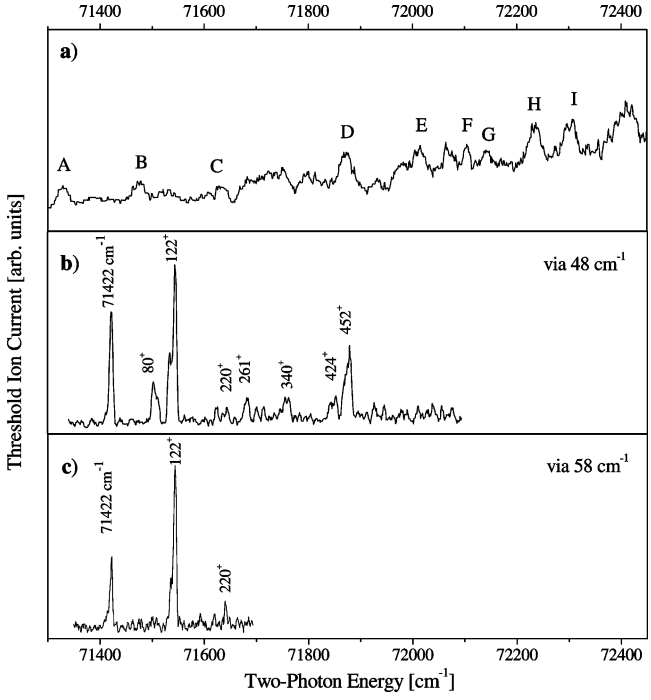

Figure 3. MATI spectra of 2-PE measured via the gauche origin (a), the 48 cm^{-1} band (b), and the 58 cm^{-1} band (c) in the S_1 electronic state. Spectrum (a) has been smoothed with 20 points averaging. The numbers in spectra (b) and (c) are the band positions relative to the 0_0^0 band at 71 422 ± 5 cm^{-1}.

characteristic vibrational structure expected for the cationic ground state. However, after extensive smoothing with 20 points averaging, some broad features appear, particularly at the high-energy end of the spectrum. The noisy spectrum has a smooth onset at around 71 400 cm^{-1}, which does not allow one to find a clear value for the adiabatic ionization energy (AIE) (see section IV). On the other hand, the MATI spectrum of the anti conformer of 2-PE obtained via the S_1 48 cm^{-1} peak (Figure 3b) shows a well-resolved vibronic structure with a strong

TABLE 1: Theoretically Predicted Harmonic Normal-Mode Vibrational Frequencies (cm^{-1}) up to 850 cm^{-1} for the Three Stable Conformations of the 2-PE Cation Calculated at the MP2/aug-cc-pVDZ and DFT M05/aug-cc-pVTZ Levels of Theory[a]

conformer **I**		conformer **II**	conformer **III**	
M05	MP2	M05	M05	MP2
56	59	50	68	53
90	93	85	89	86
148	145	133	107	102
200	234	219	234	229
240	310	247	344	292
339	332	339	355	342.95
354	344	356	371	343.04
407	386	413	387	363
440	443	460	440	377
491	508	508	516	543
529	572	523	563	609
647	622	643	646	633
760	756	753	736	761
805	779	778	796	789
816	832	802	804	807

[a] No scale factors have been applied to correct the normal-mode frequencies.

feature at 71 422 ± 5 cm^{-1} (ionization energies are given without field correction[30]), which we assign to the AIE.

The MATI spectrum via the vibronic band at 37 680 cm^{-1} (58 cm^{-1} band) in the S_1 intermediate state is shown in Figure 3c. The spectrum in Figure 3c displays the low-energy region with a better signal-to-noise ratio, obtained after averaging of nine individual scans. It features a well-pronounced vibrational structure which is close to the ground-cationic-state, D_0, vibronic pattern of the MATI spectrum measured via the band at 48 cm^{-1} in the, S_1, intermediate state (see Figure 3b). The lowest-energy peak at 71 422 ± 5 cm^{-1} coincides with the above-determined AIE of the anti conformer. The MATI spectra of Figure 3b and 3c have two characteristic peaks: the strong vibronic bond at 122 cm^{-1} and a common AIE at 71 422 ± 5 cm^{-1}.

3. Computational Results. Ab initio calculations of the cationic (D_0) ground state of 2-PE were performed with the GAUSSIAN 03 suite of programs[31] at the M05 and MP2 levels of theory using aug-cc-pVTZ and aug-cc-pVDZ basis sets, respectively. As initial geometries for the optimizations in the cationic state, we used the most stable conformers of the 2-PE monomer in the neutral ground, S_0, electronic state.[22] We used density functional theory with the recently reported hybrid M05 functional[32] for the structural optimizations, energetics, electron density distribution in the highest occupied molecular orbital (HOMO), and calculations of the normal-mode frequencies of the 2-PE cationic conformers. In this way, three stable structures for the D_0 state of 2-PE were found. Calculated harmonic vibrational frequencies yielded positive values and confirmed that they correspond to local minima. The DFT computations unveiled that two of the three neutral gauche structures survive the ionization process, while the most stable neutral conformer converges to one of the ionic gauche structures. Similarly, the two neutral anti conformers yielded the same conformer structure after ionization, with a pronounced structural change for conformer **5** and small structural changes for conformer **4**. Thus, the total number of theoretically optimized conformations of 2-PE decreases from five to three in the cationic state, one anti and two gauche structures. In addition, we employed the MP2 level of theory for optimization of the ion structures starting from the neutral ones, but there was a spin contamination

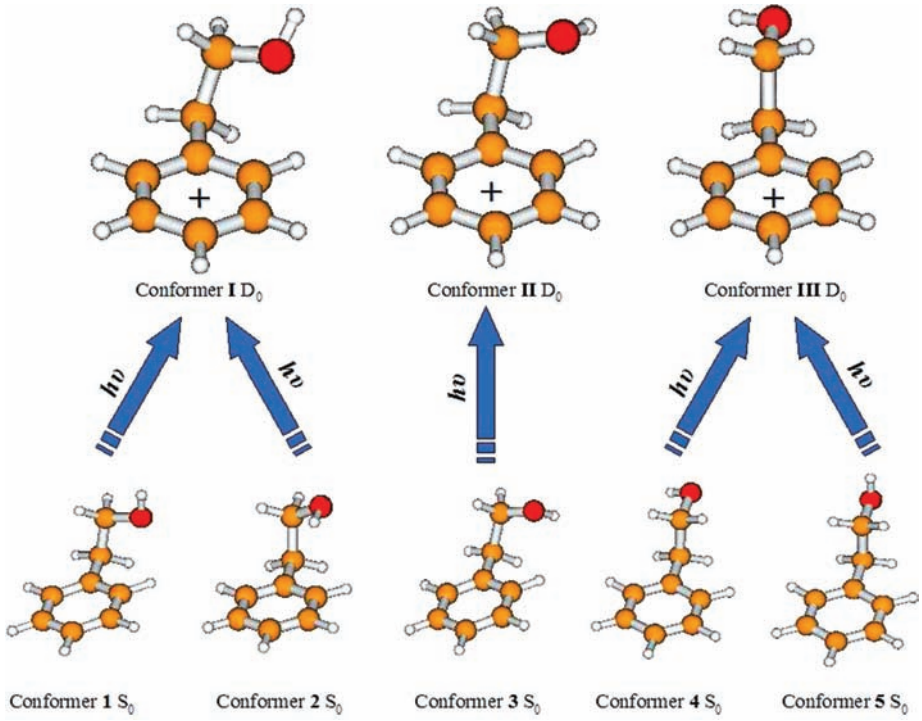

Figure 4. Conformations of the 2-PE cation (top) after ionization of the neutral conformers in the ground, S_0, electronic state (bottom) obtained from ab initio quantum chemistry full structural optimizations at the DFT M05/aug-cc-pVTZ level of theory (for explanation, see text).

TABLE 2: Electronic Origins of $S_1 \leftarrow S_0$ Transitions (cm^{-1}) for the gauche and anti Conformers of 2-PE and 2-*p*FPE[a]

conformer	theoretical	experimental	Δ
2-PE (gauche)	42 852	37 622	5230
2-*p*FPE (gauche)[b]	41 186	37 068	4118
2-PE (anti)	41 876	37 670	4206
2-*p*FPE (anti)	41 236	37 148	4088

[a] Theoretical values are from the CC2/cc-pVDZ level of theory. [b] Karaminkov, R.; Chervenkov, S.; Neuser, H. J. *J. Phys. Chem. Chem. Phys.* **2009**, *11*, 2249.

error for one of the starting gauche conformer structures. This left us with the option to use the already optimized ionic conformers (**I** and **III**) found from the M05 level of theory for further calculation of the D_0 frequencies with MP2. A comparison between the vibrational frequencies computed by the two theoretical approaches (see Table 1) with the experimental ones is made later in section IV. It is interesting to point out that none of the resulting gauche conformers in the cation features a nonclassical OH$\cdots\pi$ hydrogen bond between the terminal OH group of the side chain and the π electrons of the benzene ring. All starting geometries in the S_0 state and the respective optimized ion structures in the D_0 state are shown in Figure 4. The energy ordering obtained from the M05 calculations in the cation is as follows: conformer **II** (0 cm^{-1}), conformer **I** (+31 cm^{-1}), and conformer **III** (+667 cm^{-1}). The normal-mode frequencies up to 810 cm^{-1} for conformers **I**, **II**, and **III** calculated at the M05/aug-cc-pVTZ and MP2/aug-cc-pVDZ levels of theory are listed in Table 1.

To theoretically estimate the $S_1 \leftarrow S_0$ transition energies for the pure and *p*-fluorinated 2-PE, we performed a calculation at the CC2/cc-pVDZ level of theory using the TURBOMOLE program package.[33] The obtained energy differences in the neutral $S_1 \leftarrow S_0$ electron $\pi\pi^*$ transitions for the gauche and anti conformers of both molecules are compared with the experimental ones in the next section (see Table 2).

TABLE 3: Electronic Origins of $S_1 \leftarrow S_0$ Transitions (cm^{-1}) for Conformers I and III[a]

conformer	$\mathbf{I}_{gauche}$	$\mathbf{III}_{anti}$
$S_1 \leftarrow S_0$, 0_0^0	37 622	37 670
AIE_{exp}	70 922,[b] 69 614[c]	71 422
AIE_{theo} (M05)	66 585	67 054
AIE_{theo} (MP2)	73 471	75 379

[a] AIE_{exp}: experimental values of the adiabatic ionization energies (cm^{-1}) for conformers **I** and **III**. AIE_{theo}: theoretical values of the adiabatic ionization energies (cm^{-1}) for conformers **I** and **III** calculated at the MP2/aug-cc-pVDZ and DFT M05/aug-cc-pVTZ levels of theory. [b] AIE of the gauche conformer **I** estimated by comparison of experimental and theoretical (M05/aug-cc-pVTZ) AIEs of the anti conformer. [c] AIE of the gauche conformer **I** estimated by comparison of experimental and theoretical (MP2/aug-cc-pVDZ) AIEs of the anti conformer.

TABLE 4: Assignment of the Observed Vibronic Bands in the MATI Spectra Shown in Figure 3b and c on the Basis of the Theoretically Predicted Frequencies (cm^{-1}) for the anti Conformer of the 2-PE Cation (Conformer III in Figure 4) Calculated at the MP2/aug-cc-pVDZ Level of Theory (See Table 1)

exp. freq.	theor. freq.	assignment
80	86	β_1 bending side chain versus ring
122		Fermi resonance (For explanation, see text)
220	229	β_2 out-of-plane benzene ring bending
261		combination mode of 120 + β_1 + τ_1 (53 cm^{-1})
340	342.95	β_3 out-of-plane benzene ring bending
424		first overtone of β_2
452		combination mode of 120 + β_3

IV. Discussion

1. Comparison of MATI Spectra. In the MATI spectra of the 2-PE monomer recorded at the ion mass channel $m/z = 122$ via two vibronic bands in the first excited, S_1, electronic state (see Figure 3), we observe nicely resolved vibrational peaks for the MATI spectrum of the anti conformer (Figure 3b) and, on the other hand, a noisy MATI spectrum with an increasing

basis line for the gauche conformer. We explain this strikingly different behavior by different Franck−Condon factors resulting from structural changes of the gauche conformers taking place upon the ionization process. In the gauche structure, unfavorable Franck−Condon factors point to strong structural changes after ionization. On the other hand, the large Franck−Condon factor of the transition to the AIE of the anti conformer is due to a very small structural distortion upon ionization. This finding is supported by our quantum chemistry ab initio calculations. The DFT structural optimizations in the cation reveal that the stabilizing nonconventional OH$\cdots\pi$ bond of the neutral gauche conformer is destroyed after ionization, leading to a completely different configuration of the side chain and thus to unfavorable Franck−Condon factors for the ionization process (see Figure 4, conformer **2** → conformer **I**). On the other hand, the anti conformers **4** and **5** preserve their structures with a small change for the neutral conformer **5** (see Figure 4, conformers **4**,**5** → conformer **III**). In this case, the terminal H atom of the hydroxyl group undergoes a slight rotation leading to the same cationic conformer **III** as the one resulting from the ionization of the neutral conformer **4**. Theory predicts two stable gauche cation conformers **I** and **II** descending from the ionization of the neutral gauche conformers **1**, **2**, and **3** (see Figure 4). Theory at the DFT M05/aug-cc-pVTZ level predicts conformer **II** as the most stable one with an energy gap of only 31 cm^{-1} to conformer **I**. The small energy difference can easily result in inversion of the energy order between conformers **I** and **II** when different model theories or basis sets are employed, as it was shown for the 2-*para*-fluorophenylethanol in our recent paper.[25] Neither of the structures **I** nor **II** is expected to lead to a resolved low-frequency-range MATI signal, in view of the large structural changes after ionization of the initial most stable gauche conformer in the neutral S_1 state. In Figure 3a, in the MATI spectrum of the gauche conformer, there are some indications for vibrational peaks at higher energy. These could be due to high-frequency modes which are not dependent on the structure of the side chain and thus may have more suitable Franck−Condon factors. The peaks are broadened (the peak widths are almost three times larger than the widths of the vibronic bands in the MATI spectra recorded via the anti conformer in the S_1 intermediate electronic state), which suggests short-lived states, the short lifetime stemming most likely from intramolecular vibrational redistribution, which is encountered in flexible aromatic molecules.[34]

The MATI spectra via the bands at 48 and 58 cm^{-1} in the S_1 intermediate state presented in Figure 3b and c display a well-pronounced and very similar, yet not identical, vibrational structure. They differ, on the one hand, in the intensity ratio between the AIE and the vibronic band at 122 cm^{-1} and, on the other hand, in the absence of the peak at 80 cm^{-1} in the spectrum measured via the 58 cm^{-1} band in the intermediate S_1 electronic state (see Figure 3c). The differences can be attributed to different Franck−Condon factors corresponding to transitions via the two bands at 48 and 58 cm^{-1}, respectively. We put forward the following explanation. As already discussed in our previous publication,[22] both bands originate from the same anti conformer in the ground, S_0, electronic state. The conformer in question was assigned to be the most stable anti conformer **5** with an extended side chain. Starting from this conformer in the ground electronic state, we may access either the same conformer **5** or the other anti conformer **4** in the first excited, S_1, electronic state.[22] The presumably slightly different energies of the above two conformers in the S_1 electronic state are very likely to explain the gap of 10 cm^{-1} between the two $S_1 \leftarrow S_0$ electronic transitions. Our ab initio calculations clearly demonstrate that upon ionization, both conformers **4** and **5** converge to one and the same ionic structure. This implies that the ionization energies measured via the two bands at 48 and 58 cm^{-1} must be the same, which is confirmed by our experimental results. The explanation set out above is in accord with the UV−UV hole-burning spectra measured by Simons and co-workers[18] by tuning the probe laser frequencies onto bands 48 and 58 cm^{-1} in the S_1 intermediate state. On the basis of the obtained results, they have assigned both features as originating from one anti conformeric structure in the ground, S_0, electronic state. To rationalize the small energy gap of 10 cm^{-1}, Simons and co-workers have discussed transitions from the ground S_0 state of anti conformer **5** to two split components in the S_1 state resulting from the mixing via tunneling between the wave functions of the torsional levels of the three-fold potential corresponding to the three energy minima of the OH group (conformer **5** and two equivalent positions in conformer **4**). On the basis of the above discussion, we can assign both MATI spectra as originating from the same neutral anti conformer **5** in the ground, S_0, electronic state.

2. Adiabatic Ionization Energies. It is worth pointing out that the AIE of the anti conformation of 2-PE of 71 422 ± 5 cm^{-1}, though measured with higher resolution, does not differ much from the previous one (71 501 cm^{-1}) found by Weinkauf et al.[7] In Table 3, we compare the theoretical value of the ionization energy with that experimentally found for the anti conformer. The calculated AIE at the M05/aug-cc-pVTZ level of theory is 67 054 cm^{-1}, which is much lower than the experimental one of 71 422 cm^{-1}, but it is a good estimate. Next, we calculated the ratio of the experimental and the theoretical ionization energies to 1.065, which is almost identical to the one of 2-*p*FPE (1.068) that we found recently.[25] From the calculated AIE for the gauche conformer (66 585 cm^{-1}), at the same level of theory as that for the anti conformer, and the above correction ratio, we expect an AIE of 70 922 cm^{-1} for the gauche structure. We were not able to measure this value due to the unfavorable Franck−Condon factors for the ionization step (see above). For completeness, we calculated the AIEs for the gauche and the anti structures of 2-PE at the MP2/aug-cc-pVDZ level of theory and obtained values of 73 471 and 75 379 cm^{-1}, respectively. Compared to the experimental value for the anti structure, the theoretical one is higher by 3957 cm^{-1}, yelding a ratio of 0.947 and an expected AIE for the gauche structure of 69 614 cm^{-1}. An assignment of the next-in-energy bands is made in Table 4 by comparison between the experimental and the theoretical frequencies computed at the MP2/aug-cc-pVDZ level of theory. We attributed the experimentally detected low-frequency bands either to normal modes or to combination modes of the anti conformer. Table 1 summarizes the normal-mode frequencies obtained at the MP2/aug-cc-pVDZ and DFT M05/aug-cc-pVTZ levels of theory, and it explains well the observed band positions of the anti cationic conformation.

3. Vibrational Analysis. Regarding the normal-mode frequencies, the predictions from the MP2 and M05 theoretical models depart from each other. The agreement with the experimental frequencies is somewhat better for the MP2 level of theory, and for this reason, predicted frequencies from this calculation have been used in the analysis of the MATI spectra.

To further substantiate the conformeric origin of the MATI spectra shown in Figure 3b and c, it is worth comparing the measured band positions in the above spectra with the theoretically predicted frequencies for the presumable anti conformer **III** obtained from the ab initio quantum chemistry calculations

at the MP2/aug-cc-pVDZ level of theory listed in Table 1. On the basis of this comparison, an assignment of the observed bands is made, and the results are summarized in Table 4. The blue-shifted band centered at 80^+ cm^{-1} (see Figure 3b) is found to be the fundamental β_1 side-chain bending mode with a frequency of 86 cm^{-1}. In view of the close values of the experimental and the theoretically predicted frequencies, the mapping in this case is conclusively established. The highest-intensity band in the MATI spectra is at 122^+ cm^{-1}. There is, however, no theoretically predicted fundamental mode at that frequency. The nearest mode is the τ_2 torsional mode about the C7C8 bond with a frequency of 102 cm^{-1}. Since this mode involves only the terminus of the side chain, it is not anticipated to feature a significant anharmonicity, and for this reason, anharmonicity cannot be attributed to underlie the large difference of 20 cm^{-1}. Closely inspecting the frequencies of the fundamental modes for conformer **III** in Table 1, we put forward the following tentative assignment of the band at 122^+ cm^{-1}. The first overtone of the τ_1 torsional mode lies at 106 cm^{-1}, and it almost overlaps with the τ_2 torsional mode at 102 cm^{-1}. It is important also to highlight that both modes involve torsions of the side chain. This suggests that a coupling between the two modes is likely to occur, leading to a splitting of the band at 102 cm^{-1} and intensity redistribution of this mode over the two split components that are spread apart in a fashion like that of Fermi resonances. Thus, one of the components is pushed to a higher frequency, and in our interpretation, this should be the component giving rise to the strong band at 122^+ cm^{-1} and corresponding to a shift of 20 cm^{-1}. This model can explain fairly well the existence of the band at 122^+ cm^{-1} yet, at the same time, implicitly explain why there is no band at 102^+ cm^{-1}. Two issues, however, remain elusive, (i) where the second split component is to be found and (ii) why there is no other band with intensity comparable to the one of the band at 122^+ cm^{-1} (uneven intensity distribution). The second split component is expected to be located at 82^+ cm^{-1}. This position, however, almost coincides with the position of the fundamental β_1 side-chain bending mode and may lead to another coupling. We deem that as a net effect, a complex double resonance coupling involving the first overtone of the fundamental τ_1 torsional mode and the fundamental β_1 bending and τ_2 torsional modes may lead to the appearance of a new band pattern and intensity distribution. This mechanism, in principle, may explain that the blue-shifted component at 122^+ cm^{-1} gains intensity through the interaction of the red-shift component with the β_1 mode, ultimately resulting in intensity depletion (almost vanishing) of the red-shifted component and intensity enhancement of the blue-shifted one.

The higher-frequency vibrational bands in the MATI spectrum can be interpreted relatively straightforward either as fundamental modes, as overtones of fundamental modes, or as combination modes. The pronounced band at 220^+ cm^{-1} corresponds to the β_2 mode. The bunch of intense bands in the range from 340^+ to 362^+ cm^{-1} can be confidently mapped to the theoretically predicted (at the MP2/aug-cc-pVDZ level of theory) β_3 and C6C7 swinging fundamental modes with frequencies of 342.95 and 363 cm^{-1}, respectively. The band at 416^+ cm^{-1} is very likely to be the first overtone of the fundamental at 220^+ cm^{-1}. The last intense band in the frequency range up to 600 cm^{-1} is the band at 466 cm^{-1}. There is no fundamental mode predicted to appear in that region. Inspecting the lower frequencies, we put forward the assumption that this band is very likely to be the combination band of the highest-intensity band at 122^+ cm^{-1} and the weak band at 340^+ cm^{-1}. The reasonable assignment of the observed vibrational bands set out above is a further evidence for conformer **III** in the cationic ground, D_0, state producing the MATI spectrum.

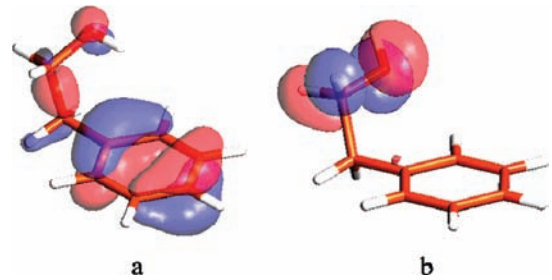

Figure 5. HOMO electron density distribution of 2-PE in the neutral ground electronic state, S_0, for (a) the most stable gauche conformer **2** and (b) in the cationic ground, D_0, electronic state for the resulting gauche conformer **I** calculated at the DFT M05/aug-cc-pVTZ level of theory.

The MATI spectrum recorded via the $S_1 \leftarrow S_0$ 0_0^0 origin band of the most stable gauche conformer **2** does not display a clear onset, and the observed peaks are located on an increasing background. However, some periodicity can be identified, which may be tentatively attributed to vibrational progressions. Two low-frequency progressions can be distinguished with frequencies of around 90 and 140 cm^{-1}. The first one is observed between bands E−F and G−H−I (see Figure 3a). The second one includes bands A−B−C and D−E. Comparing those frequencies with the theoretically obtained frequencies for the gauche conformer **I** listed in Table 1, we can tentatively map the experimental progression frequencies to the calculated ones at the M05/aug-cc-pVTZ level. The frequency of 90 cm^{-1} can be assigned to the C2C7C8 side-chain bending mode of 90 cm^{-1}. The other progression can be attributed to the side-chain torsional mode about the C7C8 bond at 148 cm^{-1}. The established correspondence provides further evidence for the origin of the MATI spectrum in discussion as stemming from the gauche conformer **I**.

4. Electron Distributions. As it was shown in our previous paper on 2-*p*FPE,[25] dispersion interactions in molecules with a nonclassical OH$\cdots\pi$ bond should be considered when using ab initio calculations for the prediction of the cationic structures. A step forward in this direction was the development of the hybrid functional M05,[23] which was specially designed to account for such weak interactions. The DFT calculations with the employment of the DFT M05/aug-cc-pVTZ level of theory predicted only three stable conformers for the cation, one anti (**III**) and two gauche ones (**I** and **II**). Figure 5 shows a comparison between the HOMO electron distribution in the neutral[22] gauche conformer **2** and that in the resulting cation gauche conformer **I** calculated at the DFT M05/aug-cc-pVTZ level of theory. A significant depletion of the π-electron density in the benzene ring in the cation is observed due to the ejected π electron together with considerable electron density relocation in the side chain. As discussed in our recent paper,[25] this can be taken as clear evidence for the presence of the OH$\cdots\pi$ bond in the neutral gauche conformer **2**.

The first excited electronic state of all conformers is the bright $^1\pi\pi^*$ state. It originates from the typical HOMO $\rightarrow$ LUMO electron transition. The orbitals involved in these transitions are illustrated in Figure 6 as obtained at the CC2/cc-pVDZ level (the ground-state geometries for the experimentally detected conformers of 2-PE and 2-*p*FPE were optimized at the MP2/cc-pVDZ level). As seen, the HOMO $\rightarrow$ LUMO transitions of the 2-*p*FPE conformers involve charge transfer from the fluorine

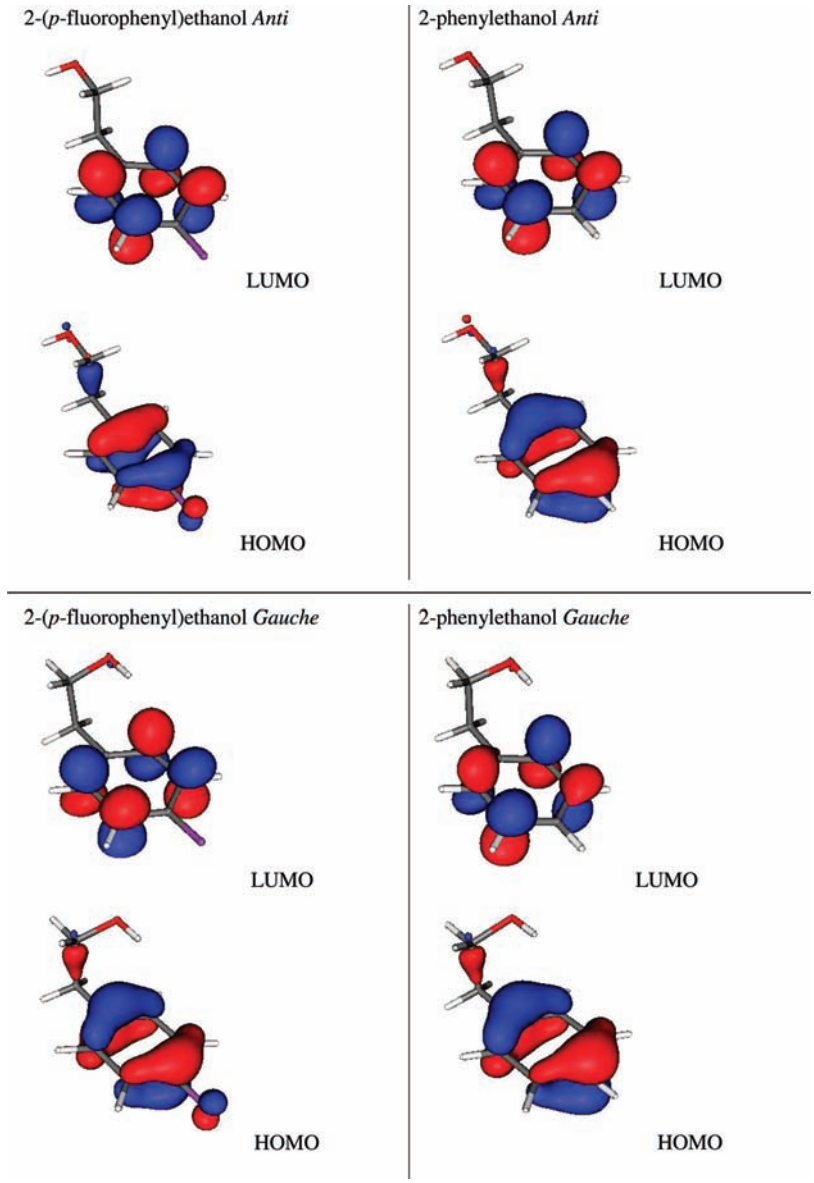

Figure 6. HOMO and LUMO molecular orbitals of the two identified gauche and anti conformers of 2-PE and 2-*p*FPE in the first excited electronic, S_1, state calculated at the CC2/cc-pVDZ level of theory.

atom to the aromatic ring. Furthermore, all transitions involve charge transfer from the C−C bond of the ethane residue to the aromatic ring. This means that the aromatic ring has an excess of electrons, and the compounds can easily liberate one electron and transform into a cation. In other words, the ionization of conformers can be easily achieved from the first excited state ($^1\pi\pi^*$). The HOMO → LUMO transitions lead to an elongation of the C−C bonds, which could finally lead to a fragmentation of 2-PE and 2-*p*FPE.

5. Fluorine Substitution Effect. To compare the present results with our recent findings,[25] we discuss the effect of fluorine substitution on the $S_1 \leftarrow S_0$ 0_0^0transition frequencies and the AIEs. The fluorine substitution effect on the spectral properties and energy potentials in π-conjugated hydrocarbons has been studied in a number of publications. Red shifts upon fluorine substitution in the benzene ring on the $S_1 \leftarrow S_0$ 0_0^0 and the AIEs are observed by comparing *para*-fluorotoluene[35] and toluene.[36] Medina et al.[37] report a fluorination effect on the excitation energies for a series of aromatic hydrocarbons and point out that fluorine substitution leads to red shifts or blue shifts depending on different positions of the F atom. A study on fluorinated polyphenylenevinylenes conveyed by Piacenza et al. showed that the excitation energy gap depends on fluorine substitution in opposite ways in the case of planar and nonplanar molecular geometries.[38] In the first case, a red shift was observed, while an increased energy gap was reported in the second case. Fluorine substitution was shown to cause a three-fold barrier to the internal rotation of the methyl group in various single-substituted fluorotoluenes.[39−43] Moreover, the magnitude of this barrier also depends on the substitution position, being smallest for *p*-fluorotoluene.[43] Similarly, Weisshaar and co-workers[44] investigated a sterically hindered six-fold symmetric methyl rotor in 2,6-difluorobenzene in S_1 and D_0 states.

In the case of 2-PE and 2-*p*FPE, a comparison between the excitation and MATI spectra in both cases brings about the following findings.

(1) The $S_1 \leftarrow S_0$ 0_0^0 origin of the gauche conformer of 2-*p*FPE is red-shifted by 555 cm^{-1} from the respective origin of the 2-PE. A similar difference of 523 cm^{-1} is found for the $S_1 \leftarrow S_0$ origins of the anti conformers.

(2) The AIEs manifest also red shifts upon fluorination, although they are now smaller (184 cm^{-1} for the anti conform-

ers). The theoretically predicted values for the AIEs of the gauche conformers (fluorinated and nonfluorinated) as well as the onsets in their threshold ion spectra also suggest a smaller red shift compared to the respective excitation spectra. However, the error in determining the AIEs in the case of gauche conformers does not allow us to determine unambiguously the exact magnitude of the red shift.

A suggestive qualitative explanation for the observed red shifts in the $S_1 \leftarrow S_0$ excitation spectrum of 2-*p*FPE can be made on the basis of the subtle interplay between the electron-withdrawing inductive effect and the electron-donating mesomeric effect.[37,45] The former tends to increase the excitation energy gap, while the latter acts to decrease it. Since the induction effect (−I) may not compete effectively with the mesomeric effect (+M) for cases of a single fluorine substitution, the net effect is an observed strong energy decrease in the $S_1 \leftarrow S_0$ transition of 2-*p*FPE. In the case of transitions to Rydberg states and/or to ionization thresholds, the mesomeric effect however does not play a significant role and depending on the relative contributions of −I and +M, the overall effect may be an increase of the energy gap (i.e., for a fluorine polysubstitution[45] where the induction effect is substantial) or to its lower decrease compared to the $S_1 \leftarrow S_0$ transition as is the case for the AIE of 2-*p*FPE.

V. Summary and Conclusions

In this work, we present new information on the prototype molecule 2-phenylethanol, resulting from $D_0 \leftarrow S_1$ MATI spectra and high-level ab initio computations. We provide clear evidence for the presence of the OH$\cdots\pi$ stabilizing bond in the neutral most abundant gauche conformer and its rupture during the ionization process accompanied by a considerable structural change in the resulting molecular cation. The disappearance of the π hydrogen bond in the cation was clearly proved experimentally by the poor vibrational structure in the MATI spectrum and an undefined AIE. This finding was confirmed by the M05/aug-cc-pVTZ theoretical calculations, which predict only three conformers in the D_0 cationic state, two gauche ones and one anti. They show distorted ionic gauche conformers resulting from the depletion of the electron density in the benzene ring after ionization of the neutral most stable gauche structures.

On the other hand, the MATI spectra measured via two different anti bands in S_1 display a well-resolved vibrational structure and are very similar, though not completely identical, with a coinciding AIE. This result combined with the findings from the M05/aug-cc-pVTZ level of theory clearly demonstrates that only one anti conformer exists in the cation whose structure does not differ very much from that of the neutral anti conformer identified in our recent high-resolution experiments.[22] The small structural changes after ionization of the anti conformer result in favorable Franck−Condon factors for the ionization process, leading to a clearly structured MATI spectrum. Furthermore, we conclude that the two different vibronic bands at 48 and 58 cm^{-1} in the S_1 state originate from the excitation of the same anti neutral conformer in the ground, S_0, electronic state and corroborate our recent assignment of the vibronic bands in the first excited electronic state. Finally, we investigated the effect of fluorine substitution on the red shifts in the $S_0 \leftarrow S_1$ 0_0^0 transitions and the AIEs by comparing the results of this work with our recent experiments on 2-*p*FPE.

In conclusion, the present investigations demonstrate that the MATI technique is a powerful tool for determination of the structure of flexible molecules in their cationic state as well as in their neutral states.

Acknowledgment. Financial support from the Deutsche Forschungsgemeinschaft is gratefully acknowledged. The authors would like to thank Prof. W. Domcke for providing computational support.

References and Notes

(1) Zwier, T. S. *J. Phys. Chem. A* **2001**, *105*, 8827.
(2) Nir, E.; Kleinermanns, K.; Grace, L.; de Vries, M. S. *J. Phys. Chem. A* **2001**, *105*, 5106.
(3) Georgiev, S.; Neusser, H. J. *J. Electron Spectrosc. Relat. Phenom.* **2005**, *142*, 207.
(4) Georgiev, S.; Neusser, H. J. *Chem. Phys. Lett.* **2004**, *389*, 24.
(5) Tong, X.; Ford, M. S.; Dessent, C. E. H.; Müller-Dethlefs, K. *J. Chem. Phys.* **2003**, *119*, 12908.
(6) Braun, J. E.; Mehnert, T.; Neusser, H. J. *Int. J. Mass. Spectrom.* **2000**, *203*, 1.
(7) Weinkauf, R.; Lehrer, F.; Schlag, E. W.; Metsala, A. *Faraday Discuss.* **2000**, *115*, 363.
(8) Dickinson, J. A.; Hockridge, M. R.; Kroemer, R. T.; Robertson, E. G.; Simons, J. P.; McCombie, J.; Walker, M. *J. Am. Chem. Soc.* **1998**, *120*, 2622.
(9) Braun, J. E.; Grebner, T. L.; Neusser, H. J. *J. Phys. Chem. A* **1998**, *102*, 3273.
(10) Helm, R. M.; Clara, M.; Grebner, T. L.; Neusser, H. J. *J. Phys. Chem. A* **1998**, *102*, 3268.
(11) Long, S. R.; Meek, J. T.; Reilly, J. P. *J. Chem. Phys.* **1983**, *79*, 3206.
(12) Müller-Dethlefs, K.; Sander, M.; Schlag, E. W. *Chem. Phys. Lett.* **1984**, *112*, 291.
(13) Zhu, L.; Johnson, P. M. *J. Chem. Phys.* **1991**, *94*, 5769.
(14) Krause, H.; Neusser, H. J. *J. Chem. Phys.* **1992**, *97*, 5923.
(15) Braun, J. E.; Neusser, H. J. *Mass Spectrom. Rev.* **2002**, *21*, 16.
(16) Huang, J.; Lin, J. L.; Tzeng, W. B. *Spectrochim. Acta, Part A* **2007**, *67*, 989.
(17) Yosida, K.; Suzuki, K.; Ishiuchi, S.; Sakai, M.; Fujii, M.; Dessent, C. E. H.; Müller-Dethlefs, K. *Phys. Chem. Chem. Phys.* **2002**, *4*, 2534.
(18) Mons, M.; Robertson, E. G.; Snoek, L. C.; Simons, J. P. *Chem. Phys. Lett.* **1999**, *310*, 423.
(19) Godfrey, P. D.; Jorissen, R. N.; Brown, R. D. *J. Phys. Chem. A* **1999**, *103*, 7621.
(20) Guchhait, N.; Ebata, T.; Mikami, N. *J. Am. Chem. Soc.* **1999**, *121*, 5705.
(21) Hockridge, M.; Robertson, E. G. *J. Phys. Chem. A* **1999**, *103*, 3618.
(22) Karaminkov, R.; Chervenkov, S.; Neusser, H. J. *J. Phys. Chem. A* **2008**, *112*, 839.
(23) Zhao, Y.; Schultz, N. E.; Truhlar, D. G. *J. Chem. Phys.* **2005**, *123*, 161103.
(24) Karaminkov, R.; Chervenkov, S.; Neusser, H. J. *Phys. Chem. Chem. Phys.* **2008**, *10*, 2852.
(25) Karaminkov, R.; Chervenkov, S.; Neusser, H. J. *Phys. Chem. Chem. Phys.* **2009**, *11*, 2249.
(26) Neuhauser, R. G.; Siglow, K.; Neusser, H. J. *J. Chem. Phys.* **1997**, *106*, 896.
(27) Gallagher, T. F. *Rydberg Atoms*; Cambridge University Press: New York, 1994; p 85.
(28) Georgiev, S.; Neusser, H. J. *J. Electron Spectrosc. Relat. Phenom.* **2005**, *142*, 207.
(29) Ernstberger, B.; Krause, H.; Kiermeier, A.; Neusser, H. J. *J. Chem. Phys.* **1990**, *92*, 5285.
(30) Chupka, W. A. *J. Chem. Phys.* **1993**, *98*, 4520.
(31) Frisch, M. J.; Trucks, G. W.; Schlegel, H. B.; Scuseria, G. E.; Robb, M. A.; Cheeseman, J. R.; Montgomery, J. A., Jr.; Vreven, T.; Kudin, K. N.; Burant, J. C.; Millam, J. M.; Iyengar, S. S.; Tomasi, J.; Barone, V.; Mennucci, B.; Cossi, M.; Scalmani, G.; Rega, N.; Petersson, G. A.; Nakatsuji, H.; Hada, M.; Ehara, M.; Toyota, K.; Fukuda, R.; Hasegawa, J.; Ishida, M.; Nakajima, T.; Honda, Y.; Kitao, O.; Nakai, H.; Klene, M.; Li, X.; Knox, J. E.; Hratchian, H. P.; Cross, J. B.; Bakken, V.; Adamo, C.; Jaramillo, J.; Gomperts, R.; Stratmann, R. E.; Yazyev, O.; Austin, A. J.; Cammi, R.; Pomelli, C.; Ochterski, J. W.; Ayala, P. Y.; Morokuma, K.; Voth, G. A.; Salvador, P.; Dannenberg, J. J.; Zakrzewski, V. G.; Dapprich, S.; Daniels, A. D.; Strain, M. C.; Farkas, O.; Malick, D. K.; Rabuck, A. D.; Raghavachari, K.; Foresman, J. B.; Ortiz, J. V.; Cui, Q.; Baboul, A. G.; Clifford, S.; Cioslowski, J.; Stefanov, B. B.; Liu, G.; Liashenko, A.; Piskorz, P.; Komaromi, I.; Martin, R. L.; Fox, D. J.; Keith, T.; Al-Laham, M. A.; Peng, C. Y.; Nanayakkara, A.; Challacombe, M.; Gill, P. M. W.; Johnson, B.; Chen, W.; Wong, M. W.; Gonzalez, C.; Pople, J. A. *Gaussian 03*, revision E.01; Gaussian, Inc.: Pittsburgh, PA, 2003.
(32) Zhao, Y.; Truhlar, D. G. *J. Phys. Chem. A* **2005**, *109*, 5656.
(33) *TURBOMOLE*, V. 5-9-1, Turbomole GmbH, Karlsruhe, 2007, www.turbomole.com.
(34) Parmenter, C. S. *Faraday Discuss. Chem. Soc.* **1983**, *75*, 7.

(35) Georgiev, S.; Chakraborty, T.; Neusser, H. J. *J. Phys. Chem. A* **2004**, *108*, 3304.
(36) Eisenhardt, C. G.; Baumgärtel, H. *Ber. Bunsen-Ges. Phys. Chem* **1998**, *102*, 12.
(37) Medina, B. M.; Beljonne, D.; Egelhaaf, H.-J.; Gierschner, J. *J. Chem. Phys.* **2007**, *126*, 111101.
(38) Piacenza, M.; Sala, F. D.; Farinola, G. M.; Martinelli, C.; Gigli, G. *J. Phys. Chem. B* **2008**, *112*, 2996.
(39) Takazawa, K.; Fujii, M.; Ito, M. *J. Chem. Phys.* **1993**, *99,* 3205.
(40) Okuyama, K.; Mikami, N.; Ito, M. *J. Phys. Chem.* **1985**, *89*, 5617.
(41) Lu, K. T.; Weinhold, F.; Weisshaar, J. C. *J. Chem. Phys.* **1995**, *102*, 6787.
(42) Okuyama, K.; Mikami, N.; Ito, M. *Laser Chem.* **1987**, *7*, 197.
(43) Walker, R. A.; Richard, E.; Lu, K. T.; SibetIii, E. L.; Weisshaar, J. C. *J. Chem. Phys.* **1995**, *102*, 8718.
(44) Walker, R. A.; Richard, E. C.; Lu, K. T.; Weisshaar, J. C. *J. Phys. Chem.* **1995**, *99*, 12422.
(45) Robin, M. B. *Higher Excited States of Polyatomic Moelcules*; Academic Press: New York, 1985; *III*.

JP908045K